Published in final edited form as:
J Immunol. 2013 January 1; 190(1): 48–57. doi:10.4049/jimmunol.1202150.

An *HLA-DRB1*-Coded Signal Transduction Ligand Facilitates Inflammatory Arthritis. A New Mechanism of Autoimmunity[1]

Joseph Holoshitz[*,§], **Ying Liu**[*], **Jiaqi Fu**[*], **Jeena Joseph**[†], **Song Ling**[*], **Alessandro Colletta**[*], **Prannda Sharma**[*], **Dana Begun**[‡], **Steven Goldstein**[‡], and **Russell Taichman**[†]

[*]Department of Internal Medicine, University of Michigan School of Medicine, Ann Arbor, Michigan, 48109, USA

[†]Department of Periodontics and Oral Medicine, University of Michigan School of Dentistry, Ann Arbor, Michigan, 48109, USA

[‡]Department of Orthopedic Surgery, University of Michigan School of Medicine, Ann Arbor, Michigan, 48109, USA

Abstract

Particular alleles of human leukocyte antigen (HLA) contribute to disease susceptibility and severity in many autoimmune conditions, but the mechanisms underlying these associations are often unknown. Here, we demonstrate that the shared epitope (SE), an *HLA-DRB1*-coded sequence motif that is the single most significant genetic risk factor for erosive rheumatoid arthritis (RA), acts as a signal transduction ligand that potently activates osteoclastogenesis, both *in vitro* and *in vivo*. The SE enhanced the production of several pro-osteoclastogenic factors and facilitated osteoclast (OC) differentiation in mouse and human cells *in vitro*. Transgenic mice expressing a human *HLA-DRB1* allele that code the SE motif demonstrated markedly higher propensity for osteoclastogenesis and enhanced bone degradation capacity *ex vivo*. In addition, the SE enhanced the differentiation of Th17 cells expressing the receptor activator for nuclear factor-κB ligand (RANKL). When the two agents were combined, IL-17 and the SE enhanced OC differentiation synergistically. When administered *in vivo* to mice with collagen-induced arthritis, the SE ligand significantly increased arthritis severity, synovial tissue OC abundance and bone erosion. Thus, the SE contributes to arthritis severity by activating an OC-mediated bone-destructive pathway. These findings suggest that besides determining the target specificity of autoimmune responses, HLA molecules may influence disease outcomes by shaping the pathogenic consequences of such responses.

INTRODUCTION

Many autoimmune diseases associate with particular human leukocyte antigen (HLA) alleles, but the mechanistic basis of these associations is often unknown. Presentation of self-antigens by HLA allele products has been implicated in some cases, but in many others, the mechanism is unclear (1). Based on structural, functional and evolutionary considerations, we have recently proposed that HLA molecules may contribute to disease pathogenesis through aberrant innate signaling by HLA allele-coded ligands (2). Here, we

[1]This study was supported by grants to JH from the US National Institutes of Health (GM088560, AR059085, AR056786, AR55170), an Innovative Basic Science Award from the American College of Rheumatology, and by a Johnson & Johnson Diversity Support grant

[§]Correspondence should be addressed to: Joseph Holoshitz, University of Michigan, 5520D MSRB1, 1150 West Medical Center Drive, Ann Arbor, MI 48109-5680, USA. Tel: 734-764-5470 Fax: 734-763-4151. jholo@umich.edu.

have put this hypothesis to the test in an experimental model of an emblematic HLA-associated disease, rheumatoid arthritis (RA).

RA is a crippling disease that afflicts 0.6–1% of the world population. The main manifestation of the disease is chronic joint inflammation and bone erosions, due to over-abundance of activated osteoclasts (OCs) in synovial tissues (3–5). Although the pathogenesis of RA is poorly understood, it is clear that genetic factors, particularly the *HLA-DRB1* locus (6,7), play a major role in disease susceptibility. It has been long observed that *HLA-DRB1* alleles coding a five amino acid sequence motif called the 'shared epitope' (SE) in the region 70–74 of the DRβ chain are found in the vast majority of RA patients (7). The SE not only confers a higher risk for RA, but also increases the likelihood of developing a more severe disease. SE-coding *HLA-DRB1* alleles are associated with earlier onset of arthritis and more severe bone erosions (8–11). Furthermore, there is evidence of gene-dose effect, where the severity of bone destruction in RA correlates positively with the number of SE-coding *HLA-DRB1* alleles (9–11).

The underlying mechanisms by which the SE affects susceptibility to - and severity of - RA are unknown. The prevailing hypothesis postulates that the SE allows presentation of putative self or foreign arthritogenic antigens (12); however, the identities of such target antigens remain elusive. We have recently demonstrated that the SE functions as a signal transduction ligand that binds to cell surface calreticulin (CRT) in a strictly allele-specific manner and activates nitric oxide (NO)-mediated pro-oxidative signaling (13–16). The SE ligand is effective in several different structural formats: in its native conformation as part of cell surface SE-positive HLA-DR molecules, or as SE-expressing HLA-DR tetramers; as cell-free non-HLA recombinant proteins genetically engineered to express the SE motif in its native α helical conformation; or as SE-positive short synthetic peptides. The functional consequences of SE ligand-activated signaling vary, dependent on the cell type. For example, in $CD8^+CD11c^+$ dendritic cells, the SE inhibits the activity of indoleamine 2,3 deoxygenase, an enzyme known to play an important role in regulatory T (Treg) cell activation. In $CD8^-CD11c^+$ dendritic cells the SE triggers production of IL-6 and IL-23, cytokines known to be involved in activation and expansion of IL-17-producing T (Th17) cells. The end result of these two complementing effects is a potent SE-activated Th17 polarization, both *in vitro* and *in vivo* (17).

Th17 cells are central players in RA pathogenesis (18). Relevant to the focus of this study, these cells have been previously shown to activate osteoclastogenesis by several mechanisms. In addition to their direct pro-osteoclastogenic effect through IL-17 production, Th17 cells express high levels of the receptor activator for nuclear factor-κB (RANK) ligand (RANKL), a key factor in osteoclastogenesis (19). Concurrently, Th17 cells activate local inflammation that involves cytokines, such as IL-6, IL-1 and TNF-α, which further increase RANKL expression and synergistically promote osteoclastogenesis (21). Finally, IL-17 can increase RANK expression on the surface of OC precursor cells and thereby sensitize them to the osteoclastogenic effect of RANKL (22).

Given the fact that the SE activates Th17 polarization, the key role of these cells in osteoclastogenesis, and the known association between the SE and erosive disease, we have undertaken to investigate whether the SE has a direct pro-osteoclastogenic effect. The rationale for this study is further strengthen by the fact that the SE is a potent activator of NO and reactive oxygen species (ROS) (13–16), signaling molecules which have been previously shown to affect the recruitment, differentiation, and activation of OCs (23–26).

Here, we demonstrate that the SE ligand has a dual effect on OC differentiation. It directly enhanced production of pro-osteoclastogenic factors and facilitated OC differentiation and

functional activation. In addition, the SE ligand enhanced $Th17^{+}RANKL^{+}$ cell differentiation. When administered *in vivo* to mice with collagen induced-arthritis (CIA), the SE ligand increased disease severity, synovial OC abundance and bone destruction.

MATERIALS AND METHODS

Mice and Reagents

Experiments were carried out in 6 to 10 weeks old DBA/1, as well as a DBA/1 mouse line carrying transgenic (Tg) collagen type II (CII)-specific TCR (D1Lac.Cg-Tg [TCRa,TCRb]24Efro/J), designated herein as "DBA/1 CII-TCR Tg mice"- kindly provided by Dr. Steven Lundy, University of Michigan Medical School. All mice were from the Jackson Laboratory (Bar Harbor, Maine). Tg mice, which endogenously express SE-positive HLA-DR4 (0401) or SE-negative HLA-DR4 (0402) alleles, were also used. These animals were kindly provided by Dr. Chella David (Mayo Clinic, MN, ref. 27) and are referred to as DRB1*0401 Tg and DRB1*0402 Tg mice, respectively. All mice were maintained and housed in the University of Michigan-Unit for Laboratory Animal Medicine facility, and all experiments were performed in accordance with protocols approved by University of Michigan Committee on Use and Care of Animals.

Macrophage colony-stimulating factor (M-CSF), receptor activator for nuclear factor κ-B ligand (RANKL), human rTGF-β and rIL-1β, as well as murine rIL-4, rIL-23, rGM-CSF, rIL-17, rIL-6, rM-CSF and rRANKL were purchased from PeproTech (Rocky Hill, NJ). Denatured chicken collagen type II (CII) was purchased from Chondrex Inc. (Redmond, WA). Complete Freund's Adjuvant (CFA) containing *Mycobacterium tuberculosis* H37Ra was purchased from BD Difco™ (Franklin Lakes, NJ). Rabbit anti-mouse CRT antibody was purchased from Thermo Scientific, MA. Rabbit BCL – X s/l (S-18) polyclonal Ig was purchased from Santa Cruz Biotechnology, CA. Rat anti-mouse IL-6 and anti-TNFα antibodies, along with isotype-matched control antibodies were purchased from R&D Systems, Inc. (Minneapolis, MN). PE-conjugated anti-mouse RANK (clone R12.31) was purchased from Biolegend (San Diego, CA). Monoclonal antibodies against mouse CD3 (clone 2C11), IL-4 (clone 11B11), IFN-γ (clone R46A2), and IL-2 (clone S4B6) were purified from the supernatants of hybridomas obtained from the University of Michigan Hybridoma Core Facility. Purified anti-mouse CD28 (clone 37.51) and murine rIL-23 were purchased from eBioscience (San Diego, CA). FITC anti-mouse CD4 (clone GK 1.5), PE or APC-conjugated anti-mouse IL-17A mAb (clone TC11-18H 10.1) and PE anti-mouse CD254 (TRANCE, RANKL - clone IKK22/5) were purchased from BioLegend (San Diego, CA). All other commercial reagents were purchased from Sigma (St Louis, MO)

Synthetic peptides were synthesized and purified (> 90%) as we previously described (14,16).

Measurement of NO, ROS and cytokine production

NO and ROS production was determined as previously described (16), using the NO probe 4,5-diaminofluorescein diacetate (DAF-2DA), or the ROS probe 2',7'-dichlorodihydrofluorescein (DCFH-DA). The fluorescence level was recorded every 5 minutes over a period of 500 minutes, using a Fusion αHT system (PerkinElmer Life Sciences) at an excitation wavelength of 488 nm and emission wavelength of 515 nm. NO and ROS levels are shown as fluorescence unites (FU); their production rates are expressed as FU/min. To measure cytokine production, cell culture supernatants were collected every 24 hours for 4 days and assayed for IL-6, IL-1α, IL1β, TNFα, IL-17 and RANKL using commercial ELISA kits (R&D Systems, Inc., Minneapolis, MN), following the manufacture's instruction.

In vitro assay for OC differentiation

Murine OCs were generated from RAW 264.7 cells or primary bone marrow cells isolated from femurs and tibias as previously described (28,29). Briefly, bone marrows cells were cultured in 48 well plates (2×10^5 per well) in α-MEM medium supplemented with 10% FBS, 100 U/ml penicillin and 100 μg/ml streptomycin, in the presence of 10 ng/ml of M-CSF alone during the first 2 days, followed by 4 additional days in the presence of 10 ng/ml of M-CSF, plus 20 ng/ml of RANKL. To differentiate OC from RAW 264.7, cells were cultured in the same way (2×10^4 per well), except that RANKL was added at a concentration of 20 ng/ml, for 5–6 days. Human OCs were differentiated from peripheral blood mononuclear cells (PBMCs) isolated from healthy blood donors as previously described (30). PBMCs were cultured for 7 days in 100 ng/ml of M-CSF and 100 ng/ml of RANKL -supplemented in 10% FCS DMEM. To quantify the number of OCs, cultures were fixed and stained for tartrate-resistant acid phosphatase (TRAP) activity using an acid phosphatase kit (Kamiya Biomedical Company, Seattle, WA) according to the manufacturer's instructions. TRAP-positive multinucleated OCs (>3 nuclei) were counted using a tissue culture inverted microscope (30).

In vitro bone resorption assays

Degradation of osteoblast-derived bone matrix was quantified as previously described (31) with some modifications. Briefly, 12,000 osteosarcoma cells (SaOS-2) per well were cultured in McCoy's 5A medium supplemented with 15% FBS in 48-well polystyrene culture plates. When cultures reached 80–90% confluence, the medium was changed to osteoblast differentiation medium (α-MEM, Gibco), containing 10% FBS, 2mM glutamine, 300 mM ascorbic acid, 10 mM β-glycerol phosphate. After 20–25 days, osteoblasts were removed using 15 mM NH_4OH. Mouse BMCs (200,000 cells/well in 48-well plates) were plated on the matrix in an OC differentiation medium as above. At different time points, cells were removed using 15mM NH_4OH and matrix was stained with Von Kossa dye. Photographs of individual wells were taken using a transmitted light microscope and matrix abundance was quantified by Image-J software.

To determine *ex-vivo* bone degradation, 5-mm-diameter bovine cortical bone disks were prepared and studied as described (32) with some modifications. Briefly, disks were washed and sonicated in distilled water, and stored dry at room temperature. Before use, bone disks were sterilized by immersion in ethanol and placed under UV light for 30 min. Single disks were placed in individual wells with 0.5 ml alpha MEM + 10 ng/ml M-CSF + 20 ng/ml RANKL. Mouse BMCs, 400,000 cells per well, were incubated for 10 days with replenishment of fresh media every other day. At the end of incubation, bone disks were removed and stained for TRAP and number of OC per disk was determined as above. Cells and debris were then removed by 2 bursts of 15-second sonication in concentrated ammonium hydroxide. Disks were stained with 1% toluidine blue for 30 seconds, and resorption pits were counted by scanning the entire surface of each disk with a reflected light microscope.

Differentiation of Th17 cells *in vitro*

Splenocytes, (2×10^5 per well) were cultured in 96 well plates in IMDM (Gibco, Carlsbad, CA) supplemented with 2 mM L-glutamine, 10% FBS, 1% Penicillin-Streptomycin, 10 mM HEPES buffer solution and 50 mM 2-mercaptoethanol, in the presence of Th17-polarazing cocktail containing: anti-IL4 (2 μg/ml), anti-IFNγ (2 μg/ml), rhTGFβ (1 ng/ml), rmIL-6 (20 ng/ml), rmIL-23 (10 ng/ml), rhIL-1β (10 ng/ml), anti-CD3 (2 μg/ml) and anti-CD28 (5 μg/ml). Cells were stimulated with 50 μg/ml of SE-positive 65-79*0401, SE-negative 65-79*0402 or PBS and cultured for 5 days. After 5 days, cells were stimulated with PMA (5 ng/ml) and ionomycin (500 ng/ml) for the last 6 hours of culture. Brefeldin A (10 μg/ml)

was added to the culture for the last 5 hrs. Cells were then harvested and stained for surface marker using FITC anti-mouse CD4 and isotype controls followed by fixation and permeabilization using a Cytofix/Cytoperm™ kit (eBioscience, San Diego, CA). Intracellular staining was performed using APC-conjugated anti-mouse IL-17A mAb and PE-conjugated anti-mouse RANKL. Mean florescence intensity and percentages of stained cells were determined by FACS analysis.

In other experiments, lymph-node or splenic cells isolated from CIA mice were re-stimulated *ex vivo* for 5 days in the presence or absence of denatured chicken CII (100 μg/ml) before Th17 abundance was determined by flow cytometry as above.

CIA induction and *in vivo* peptide administration

DBA/1 CII-TCR Tg mice (6–10 week old) were immunization with chicken CII in CFA. In brief, 50 μl of an emulsion containing 100 μg of CII in 25 μl of 0.05 M acetic acid and 25 μl of CFA was injected intradermally at the base of the tail. In addition, mice were injected twice per week intraperitoneally with 100 μg of either SE-positive peptide 65-79*0401, or SE-negative peptide 65-79*0402 in 50 μl of PBS. Other groups were injected with 50 μl of PBS alone. Mice were monitored and paw swelling was determined as previously described (33), using a visual scoring system on a 4-point scale for each paw: 0 = no arthritis, 1 = swelling and redness confined to digits, 2 = minor swelling and redness spreading from the digits to the distal paw, and 3 = major swelling and redness extending proximally from the paw.

Joint tissue studies

Limbs were dissected and decalcified in 10% EDTA for 14 days at 4°C. After decalcification, the specimens were processed for paraffin embedding and serial sectioned. The histological sections were deparaffinized, rehydrated and stained with hematoxylin and eosin (H&E), or for TRAP activity using an acid phosphatase kit (Kamiya Biomedical Company, Seattle, WA). To determine OC abundance, TRAP-positive multinucleated cells were counted. Data, shown as “OC count”, represent mean ± SEM of the total number of OCs in front and rear paws + knees.

Radiological imaging

Bone damage was evaluated by radiography and micro-computed tomography (micro-CT). Front and hind limbs from arthritic mice were dissected, fixed in 10% formalin and stored in 70% ethanol. Limbs were scanned *ex vivo* by a micro-CT system (eXplore Locus SP, GE Healthcare Pre-Clinical Imaging, London, ON) in distilled water. The protocol included the source powered at 80 kV and 80 μA. In addition to a 0.508 mm Al filter, an acrylic beam flattener was used to reduce beam hardening artifact (34). Exposure time was defined at 1600 ms per frame with 400 views taken at increments of 0.5°. With 4 frames averaged and binning at 2×2, the images were reconstructed with an 18 μm isotropic voxel size.

Regions of interest were defined through a spline-fitting algorithm to create separate masks for the carpals, tarsals, calcaneus, talus, or phalanges. The global threshold for cortical bone was defined at 2000 HU and 1200 HU for trabecular bone. Image analysis was run using MicroView 2.2 Gold (GE Healthcare Pre-Clinical Imaging, London, ON). Hounsfield values were mapped using a color gradient to qualitatively analyze density patterns. Tissue mineral content (TMC), tissue mineral density (TMD), and bone volume fraction (BVF) were quantified for each region, as previously described (34).

Radiographs were taken using a microradiography system (Faxitron X-ray Corporation, Wheeling, IL, USA) with the following operating settings: 27 peak voltage, 2.5 mA anode

current, and an exposure time of 2.6 seconds. Coded radiographs were evaluated by an experienced rheumatologist who was blinded to the treatment. The presence of bone destruction was assessed separately for front and rear paws and scored on a scale of 0–5, ranging from no damage to complete destruction of the joints as previously described (35).

Statistical analysis

Data are expressed as mean ± SEM from triplicate samples. All experiments were repeated at least 3 times. Unless otherwise stated, all statistical analyses were performed using a 2-tailed Student's T-test (*, $p < 0.05$; **, $p < 0.01$)

RESULTS

The SE activates NO and ROS production, and facilitates OC differentiation in pre-OCs

We have previously demonstrated that the SE ligand triggers NO and ROS production in several cell types (13–16). Given the known effect of NO and ROS on OCs (23–26), we examined whether the SE could activate NO and ROS signaling in the OC precursor cell line RAW 264.7. To this end, cells were treated with the SE ligand 65-79*0401, a SE-negative control peptide 65-79*0402, or PBS, and NO and ROS production was measured. As seen in Figures 1A and 1B, the SE ligand 65-79*0401 activated markedly higher NO and ROS production, compared to the control peptide or PBS. Activation of NO and ROS signaling in RAW 264.7 cells by the SE ligand, similar to its effect in fibroblasts (16), depended on cell surface CRT (Figures 1C and 1D).

Because NO and ROS possess pro-osteoclastogenic effects (23–26) we sought to determine whether the SE could affect OC differentiation. To this end, RAW 264.7 cells were cultured with different concentrations of the SE-positive ligand 65-79*0401, a control SE-negative peptide 65-79*0402, or PBS. OC abundance was determined by quantification of multinucleated, TRAP-positive cells. The SE ligand 65-79*0401 activated increasing OC differentiation over time (Figure 1E), with an optimum concentration of 50 μg/ml (Figure 1F). Under these conditions the SE ligand could activate significantly higher differentiation rates even in the absence of exogenous RANKL; however, more potent effect was seen in the presence of the recombinant protein (Figures 1G and 1H). To determine whether the effect was specifically dependent on the SE sequence motif (QKRAA, QRRAA, or RRRAA), we tested a panel of SE-positive or –negative synthetic peptides. As can be seen in Table 1, peptide-activated osteoclastogenesis was strictly dependent on the SE sequence motif.

The SE facilitates primary cell OC differentiation and bone degradation *in vitro*

To examine the effect of the SE ligand on primary cells, OC differentiation was induced in bone marrow cells (BMCs) derived from DBA/1 mice as previously described (28,29). Differentiation of OCs from BMCs was carried out in the presence of the SE ligand 65-79*0401, a SE-negative control peptide 65-79*0402, or PBS as above. After 6 days, cells were stained for TRAP and OCs were counted. As seen in Figure 2A, the SE significantly increased OC differentiation. The SE ligand facilitated OC differentiation in healthy human peripheral blood mononuclear cells (PBMCs) as well. To date, 11 such blood samples were tested. In all but 2 cases, the SE-positive peptide 65-79*0401 produced strong pro-osteoclastogenic effects. A representative experiment is shown in Figure 2B.

An endogenously-expressed SE had a similar effect to that seen with an exogenously added synthetic ligand. Fresh BMCs isolated from naïve DRB1*0401 Tg (transgenic mice expressing human HLA-DR molecules coded by the SE-positive *HLA-DRB1*04:01* allele; reference 27) showed higher constitutive abundance of TRAP-positive mononuclear (pre-

OC) cells, compared to BMCs from DRB1*0402 Tg, expressing a SE-negative HLA-DR molecule (Figure 2C). Furthermore, after 6 days in OC-differentiating culture conditions, BMCs from DRB1*0401 Tg mice showed a significantly higher number of fully differentiated OCs (Figure 2D). The osteoclastogenic propensity of DRB1*0401 Tg BMCs was accompanied by higher capacity to degrade artificial bone matrix (Figure 2E) and bovine bone disks (Figure 2F) *ex vivo.* Thus the SE ligand facilitates *in vitro* differentiation of OCs and enhances their bone-degrading functional activity.

The SE activates production of pro-osteoclastogenic factors

RA synovial fluids and tissues express high levels of inflammatory cytokines, such as IL-1, IL-6, IL-17 and TNF-α, which play important roles in bone destruction (21,36). To determine the effect of the SE on pro-osteoclastogenic cytokine production, we cultured RAW 264.7 (Figure 3A), or primary mouse BMCs (Figure 3B) in OC-differentiating conditions, in the presence of the SE ligand 65-79*0401, a SE-negative control peptide 65-79*0402 or PBS. Cytokine levels were measured in culture supernatants by ELISA. As seen in Figures 3A and 3B, the SE ligand significantly augmented IL-6 and TNF-α production by both RAW 264.7 and BMCs. There was no increased production of IL-1α, or IL-1β in either RAW 264.7 cells or BMCs. Additionally, the SE ligand did not increase IL-17 levels in BMC cultures, or RANKL in RAW 264.7 cells.

Both IL-6 and TNFα enhance osteoclastogenesis, and their levels are substantially elevated in the synovial fluid of RA patients (37,38). We therefore examined whether these cytokines contribute to SE-activated osteoclastogenesis, using neutralizing antibodies. Both anti-IL-6 (Figure 3C) and anti-TNFα (Figure 3D) neutralizing antibodies inhibited SE-activated mouse bone marrow-derived OC generation. Thus, we conclude that IL-6 and TNFα play a role in SE-activated osteoclastogenesis.

OC differentiation depends largely on an interaction between RANKL and its signaling receptor, RANK (39). OC precursor cells can be sensitized to RANKL by increasing RANK expression, with resultant increased OC generation. We therefore undertook to determine whether the SE increases the expression of RANK on OC precursor cells. RAW 264.7 cells were treated with the SE ligand 65-79*0401, SE-negative peptide 65-79*0402, or PBS in the presence of low concentration (10 ng/ml) of recombinant RANKL. RANK expression was significantly higher on RAW 264.7 cell-differentiated OCs when they were cultured in the presence of the SE ligand (Figure 3E).

Th17 cells possess a pro-osteoclastogenic effect, which is attributed partly to their own RANKL expression, and partly to IL-17 production. We have previously demonstrated that the SE ligand enhances Th17 cell differentiation (17). Accordingly, experiments to determine whether the SE could activate Th17-dependent osteoclastogenesis were performed. SE-stimulated DBA/1 splenocytes demonstrated significantly higher abundance of RANKL-expressing Th17 cells, compared to splenic cells stimulated with the control peptide or PBS (Figure 3F). Furthermore, under suboptimal osteoclastogenic tissue culture conditions, the SE ligand interacted with IL-17 (Figure 3G). As can be seen, in limiting concentrations of RANKL (5 ng/ml) and IL-17 (0.1–1.0 ng/ml) the SE ligand and IL-17 had a synergistic pro-osteoclastogenic effect on mouse BMCs. Thus, our results suggest that in addition to its direct T cell-independent effect on OCs, the SE exerts a Th17 cell-mediated pro-osteoclastogenic effect by enhancing the differentiation of RANKL-expressing IL-17 producing T cells.

Arthritogenic effects of the SE *in vivo*

To determine the effect of the SE *in vivo*, we studied CIA. CII-immunized DBA/1 CII-TCR Tg mice were injected intra-peritoneally with SE-positive peptide 65-79*0401, SE-negative control peptide 65-79*0402 or PBS. As can be seen in Figure 4, SE-treated CIA mice showed higher Th17 abundance in regional lymph nodes, compared to mice treated with the control peptide (Figure 4A and 4B). *Ex vivo* lymph node cell expansion under Th17 differentiating conditions in the presence or absence of CII showed selective expansion of CII-specific Th17 cells in mice treated with the SE, compared to mice treated with the control peptide (Figures 4C and 4D).

Importantly, treatment with the SE ligand significantly facilitated disease onset (Figure 5A) and increased joint swelling (Figure 5B), compared to mice injected with the control peptide or PBS. The tissue swelling effect was transient, yet clearly significant, particularly during day 21–35 after immunization ($p = 8.7 \times 10^{-5}$, in a paired Student t-test). Radiologic analysis showed that mice treated with the SE ligand had more severe erosive bone damage when compared to mice treated with the control peptide (Figures 5C and 5D). Micro-CT-based bone mineral density imaging showed reduced bone mass in SE-treated mice, particularly in the ankles, with the most significant loss found in the calcaneus (Figures 5E and 5F).

Histologic examination of arthritic joints revealed significantly higher abundance of OCs in SE-treated mice (Figures 6A and 6B). Additionally, there was a higher abundance of TRAP-positive mononuclear (pre-OC) cells in the bone marrow of SE-treated mice (Figure 6C). Upon *ex vivo* differentiation for 6 days, BMCs harvested from SE-treated CIA mice formed significantly higher numbers of OCs (Figure 6D).

DISCUSSION

RA, an emblematic HLA-associated autoimmune disease, is characterized by extensive bone damage, which for unknown reasons is more severe in patients carrying SE-coding *HLA-DRB1* alleles (9–11). This study identified the SE as a signal transduction ligand that can potently activate a bone-destructive pathway, both *in vitro* and *in vivo*. Our previous studies have demonstrated that the SE acts as a signal transduction ligand that interacts with cell surface CRT and activates immune dysregulatory events both *in vitro* and *in vivo* (13–17). Here we demonstrate, for the first time, that the SE ligand has direct arthritogenic effects. These findings have several important implications for our understanding of the mechanisms governing autoimmune arthritis, as discussed below.

Our results demonstrated that similar to its effect in fibroblasts (16), SE signaling in OCs depended on interaction with its receptor, CRT. We have previously demonstrated that the SE ligand binds to a particular site on cell surface CRT (40) in an allele-specific manner, activates NO and ROS signaling and leads to distinct functional consequences, dependent on the cell type with which it interacts. For example, in $CD8^+$ dendritic cells the SE signal inhibits indoleamine 2,3 deoxygenase activation, while in $CD8^-$ dendritic cells, it activates production of Th17-polarizing cytokines. The end result of this dual effect is immune dysregulation with Th17 polarization (17). Here we demonstrated that similar to fibroblasts, lymphocytes and dendritic cells, the SE ligand interacted with cell surface CRT on OCs and activated NO and ROS production. Different from other cell types, however, in OCs, these signaling events resulted in a distinct lineage-specific functional effect (osteoclastogenesis). Thus, consistent with our previous observations, cell surface CRT is the SE signal transducing receptor in many cell types. While activation of the CRT-mediated pathway by the SE triggers lineage-invariant signaling events, the functional consequences are lineage-specific.

Recent studies have implicated Th17 cells in the pathogenesis of RA and CIA, and demonstrated that the signature cytokine of Th17 cells, IL-17, can activate OC differentiation and activity (19–21). Based on this prior knowledge, and our own data (17), it would have been reasonable to hypothesize that the SE ligand may increase bone damage secondary to its effect on Th17 polarization. Unexpectedly however, we discovered here that the SE had two distinct effects: enhancement of RANKL-expressing Th17 cell differentiation on the one hand, and direct effect on OC differentiation in the absence of T cells (*i.e.* in RAW 264.7 cells) on the other. It is noteworthy that SE effect was enhanced in the presence of IL-17, suggesting that although the SE had 2 distinct effects, the two mechanisms operate synergistically. Importantly, the SE ligand stimulated osteoclastogenesis in human cell cultures as well, indicating the effect is species-unrestricted.

SE-activated osteoclastogenesis was found to be mediated by previously identified pathways. For example, SE effect involved production of intracellular signaling molecules (NO and ROS) and cytokines (IL-6 and TNFα) that have been previously found to participate in osteoclastogenesis. The unifying effector mechanism behind SE pro-osteoclastogenic effects is unknown, but IL-6 is a plausible candidate, since it has been previously found to mediate SE-activated Th17 polarization (17) and in the presence of soluble IL-6R was shown to activate osteoclastogenesis (41). Thus, the data in Figure 3 suggest that the seemingly unconnected SE-induced events may all be mediated by IL-6. Obviously, deciphering cause-effect relationships in a multi-lineage, multi-factorial system such as SE-induced osteoclastogenesis requires further studies.

Accumulating evidence indicates that bone damage in RA affects both local and remote skeletal tissues (42). In this study SE bone effects were seen in articular, peri-articular and extra-articular bone sites. Radiological data confirmed that SE-activated OC accumulation *in vivo* was associated with greater degree of articular erosion. In addition, imaging studies demonstrated diffuse bone resorption in peri-articular (*e.g.* carpal bones) and extra-articular (*e.g.* calcaneus) tissues as well. In addition, the SE ligand potently activated *in vitro* osteoclastogenesis in BMCs collected from naïve mice. Furthermore, freshly isolated BMCs from SE-treated CIA mice showed higher abundance of pre-OCs, and higher susceptibility to osteoclastogenesis when cultured *ex-vivo* in OC-differentiating conditions. When taken together, these findings indicate that SE ligand-activated bone damaging effects *in vivo* extended beyond the joint compartment, resembling the bone damage distribution seen in RA.

Osteoclastogenesis, increased NO and ROS levels and Th17 over-abundance have all been implicated in many autoimmune conditions. Then, how does the SE lead to the development of RA rather than other diseases? Our model (2,13,43,44) proposes that RA disease onset depends on a constellation of events involving particular cell lineages and target tissues that are affected by SE signaling, as well as the relative potency of the signals and cross-talk with other pathways. Additionally, RA development depends on additional genes besides SE-coding *HLA-DRB1* alleles. Finally, non-genetic influences (*e.g.* environmental factors) play important roles in RA development. Importantly, it has been previously shown that in RA, the SE and cigarette smoking interact synergistically to increase disease-risk (45). Thus, many factors besides the presence of a SE are required in order to jointly trigger disease onset in RA.

The findings of this study lend important support to the SE Ligand hypothesis (2,13,43,44). As mentioned above, the underlying mechanism of SE-RA association is unknown. Our *in vitro* and *in vivo* studies to date (13–17) have indirectly supported the SE Ligand hypothesis. However, direct evidence to conclusively implicate the SE as a signal transduction ligand in

the pathogenesis of arthritis has been missing. By demonstrating the effect of the SE in CIA and identifying the pathophysiologic basis of that effect, this study helps to determine the functional role of the SE. Our data demonstrated that the SE ligand had potent pathogenically-relevant effects at μM-range concentrations of a synthetic cell-free molecule which does not possess antigen-presentation properties. Consistent with this, we have recently developed a bio-stable peptidomimetic SE ligand that is approximately 100,000 times more active on a molar basis than the SE ligand used here both in signaling (46) and osteoclastogenesis (manuscript in preparation).

The newly identified pathogenic mechanism of SE may provide answers to several questions that antigen presentation cannot clearly explain. For example, RA concordance rate in monozygotic twins (47) and bone damage severity (9–11) both correlate directly with the number of SE-coding alleles. Such dose-dependent patterns are more consistent with signal transduction than antigen presentation. Further, in addition to its well-known effect on RA, the SE has been found to associate with bone erosions in non-RA conditions, such as psoriatic arthritis (48), SLE (49) and periodontal disease (50). Those conditions do not share a common pathogenesis, or a putative target antigen. It is therefore conceivable that it is the SE ligand activity, rather than antigen presentation that renders individuals carrying certain *HLA-DRB1* alleles susceptible to excessive bone damage in a variety of clinical settings. Our finding that naïve transgenic mice carrying the SE-coding *HLA-DRB1* allele have higher inherent propensity for osteoclastogenesis is consistent with this scenario.

In conclusion, we identified SE, a sequence motif best known for its association with severe RA, as a signaling ligand that facilitates OC-mediated bone damage. Beyond uncovering a functional effect of the single most significant genetic risk factor in RA, whose mechanism of action has eluded the field for over 2 decades (6,7), these findings introduce a novel paradigm that could provide a plausible mechanistic context to the enigmatic association of HLA alleles with a wide range of diseases (1).

Acknowledgments

We thank Dr. Chella David for providing HLA-DR4 Tg mice, Hahyung Kim for technical assistance, and Gail Quaderer for administrative support.

Abbreviations used in this manuscript

CIA	collagen-induced arthritis
CII	collagen type II
CRT	calreticulin
CT	computerized tomography
DAF-2DA	4,5-diaminofluorescein diacetate
DCFH-DA	2',7'-dichlorodihydrofluorescein
FU	fluorescence units
OC	osteoclast
RA	rheumatoid arthritis
RANK	receptor activator for nuclear factor-κB ligand
RANKL	RANK ligand
ROS	reactive oxygen species

SE	shared epitope
Tg	transgenic
TRAP	tartrate-resistant acid phosphatase

REFERENCES

1. Klein J, Sato A. The HLA system. Second of two parts. N. Eng. J. Med. 2000; 343:782–786.
2. de Almeida DE, Holoshitz J. MHC molecules in health and disease: At the cusp of a paradigm shift. Self Nonself. 2011; 2:43–48. [PubMed: 21776334]
3. Bromley M, Woolley DE. Histopathology of the rheumatoid lesion. Identification of cell types at sites of cartilage erosion. Arthritis Rheum. 1984; 27:857–863. [PubMed: 6466394]
4. Fujikawa Y, Shingu M, Torisu T, Itonaga I, Masumi S. Bone resorption by tartrate-resistant acid phosphatase-positive multinuclear cells isolated from rheumatoid synovium. Br J Rheumatol. 1996; 35:213–217. [PubMed: 8620294]
5. Gravallese EM, Manning C, Tsay A, et al. Synovial tissue in rheumatoid arthritis is a source of osteoclast differentiation factor. Arthritis Rheum. 2000; 43:250–258. [PubMed: 10693863]
6. Stastny P. HLA-D and Ia antigens in rheumatoid arthritis and systemic lupus erythematosus. Arthritis Rheum. 1978; 21:S139–S143. [PubMed: 307389]
7. Gregersen PK, Silver J, Winchester RJ. The shared epitope hypothesis. An approach to understanding the molecular genetics of susceptibility to rheumatoid arthritis. Arthritis Rheum. 1987; 30:1205–1213. [PubMed: 2446635]
8. Gonzalez-Gay MA, Garcia-Porrua C, Hajeer AH. Influence of human leukocyte antigen-DRB1 on the susceptibility and severity of rheumatoid arthritis. Semin Arthritis Rheum. 2002; 31:355–360. [PubMed: 12077707]
9. Mattey DL, Hassell AB, Dawes PT, et al. Independent association of rheumatoid factor and the HLA-DRB1 shared epitope with radiographic outcome in rheumatoid arthritis. Arthritis Rheum. 2001; 44:1529–1533. [PubMed: 11465703]
10. Plant MJ, Jones PW, Saklatvala J, Ollier WE, Dawes PT. Patterns of radiological progression in early rheumatoid arthritis: results of an 8 year prospective study. J Rheumatol. 1998; 25:417–426. [PubMed: 9517757]
11. Weyand CM, Goronzy JJ. Disease mechanisms in rheumatoid arthritis: gene dosage effect of HLA-DR haplotypes. J Lab Clin Med. 1994; 124:335–338. [PubMed: 8083576]
12. Wucherpfennig KW, Strominger JL. Selective binding of self peptides to disease-associated major histocompatibility complex (MHC) molecules: a mechanism for MHC-linked susceptibility to human autoimmune diseases. J Exp Med. 1995; 181:1597–1601. [PubMed: 7722439]
13. Holoshitz J, Ling S. Nitric oxide signaling triggered by the rheumatoid arthritis shared epitope: a new paradigm for MHC disease association? Ann N Y Acad Sci. 2007; 1110:73–83. [PubMed: 17911422]
14. Ling S, Lai A, Borschukova O, Pumpens P, Holoshitz J. Activation of nitric oxide signaling by the rheumatoid arthritis shared epitope. Arthritis Rheum. 2006; 54:3423–3432. [PubMed: 17075829]
15. Ling S, Li Z, Borschukova O, Xiao L, Pumpens P, Holoshitz J. The rheumatoid arthritis shared epitope increases cellular susceptibility to oxidative stress by antagonizing an adenosine-mediated anti-oxidative pathway. Arthritis Res Ther. 2007; 9:R5. [PubMed: 17254342]
16. Ling S, Pi X, Holoshitz J. The rheumatoid arthritis shared epitope triggers innate immune signaling via cell surface calreticulin. J Immunol. 2007; 179:6359–6367. [PubMed: 17947714]
17. de Almeida DE, Ling S, Pi X, Hartmann-Scruggs AM, Pumpens P, Holoshitz J. Immune dysregulation by the rheumatoid arthritis shared epitope. J Immunol. 2010; 185:1927–1934. [PubMed: 20592276]
18. Shahrara S, Huang Q, Mandelin AM 2nd, Pope RM. TH-17 cells in rheumatoid arthritis. Arthritis Res Ther. 2008; 10:R93. [PubMed: 18710567]

19. Sato K, Suematsu A, Okamoto K, et al. Th17 functions as an osteoclastogenic helper T cell subset that links T cell activation and bone destruction. J Exp Med. 2006; 203:2673–2682. [PubMed: 17088434]
20. Kotake S, Udagawa N, Takahashi N, et al. IL-17 in synovial fluids from patients with rheumatoid arthritis is a potent stimulator of osteoclastogenesis. J Clin Invest. 1999; 103:1345–1352. [PubMed: 10225978]
21. Takayanagi H. Osteoimmunology and the effects of the immune system on bone. Nat Rev Rheumatol. 2009; 5:667–676. [PubMed: 19884898]
22. Adamopoulos IE, Chao CC, Geissler R, et al. Interleukin-17A upregulates receptor activator of NF-kappaB on osteoclast precursors. Arthritis Res Ther. 2010; 12:R29. [PubMed: 20167120]
23. Lee NK, Choi YG, Baik JY, et al. A crucial role for reactive oxygen species in RANKL-induced osteoclast differentiation. Blood. 2005; 106:852–859. [PubMed: 15817678]
24. Rahnert J, Fan X, Case N, et al. The role of nitric oxide in the mechanical repression of RANKL in bone stromal cells. Bone. 2008; 43:48–54. [PubMed: 18440890]
25. Kim MS, Yang YM, Son A, et al. RANKL-mediated reactive oxygen species pathway that induces long lasting Ca2+ oscillations essential for osteoclastogenesis. J Biol Chem. 2010; 285:6913–6921. [PubMed: 20048168]
26. Garrett IR, Boyce BF, Oreffo RO, Bonewald L, Poser J, Mundy GR. Oxygen-derived free radicals stimulate osteoclastic bone resorption in rodent bone in vitro and in vivo. J Clin Invest. 1990; 85:632–639. [PubMed: 2312718]
27. Taneja V, Behrens M, Basal E, et al. Delineating the role of the HLA-DR4 "shared epitope" in susceptibility versus resistance to develop arthritis. J Immunol. 2008; 181:2869–2877. [PubMed: 18684978]
28. Kobayashi K, Takahashi N, Jimi E, et al. Tumor necrosis factor alpha stimulates osteoclast differentiation by a mechanism independent of the ODF/RANKL-RANK interaction. J Exp Med. 2000; 191:275–286. [PubMed: 10637272]
29. Koga T, Inui M, Inoue K, et al. Costimulatory signals mediated by the ITAM motif cooperate with RANKL for bone homeostasis. Nature. 2004; 428:758–763. [PubMed: 15085135]
30. Kim J, Jung Y, Sun H, et al. Erythropoietin mediated bone formation is regulated by mTOR signaling. J Cell Biochem. 2012; 113:220–228. [PubMed: 21898543]
31. Lutter AH, Hempel U, Wolf-Brandstetter C, Garbe AI, Goettsch C, Hofbauer LC, Jessberger R, Dieter P. A novel resorption assay for osteoclast functionality based on an osteoblast-derived native extracellular matrix. J Cell Biochem. 2010; 109:1025–1032. [PubMed: 20108253]
32. Yang CR, Wang JH, Hsieh SL, Wang SM, Hsu TL, Lin WW. Decoy receptor 3 (DcR3) induces osteoclast formation from monocyte/macrophage lineage precursor cells. Cell Death Differ. 2004; 11(Suppl 1):S97–S107. [PubMed: 15002040]
33. Wooley PH, Luthra HS, Stuart JM, David CS. Type II collagen-induced arthritis in mice. I. Major histocompatibility complex (I region) linkage and antibody correlates. J Exp Med. 1981; 154:688–700. [PubMed: 6792316]
34. Meganck JA, Kozloff KM, Thornton MM, Broski SM, Goldstein SA. Beam hardening artifacts in micro-computed tomography scanning can be reduced by X-ray beam filtration and the resulting images can be used to accurately measure BMD. Bone. 2009; 45:1104–1116. [PubMed: 19651256]
35. Joosten LA, Helsen MM, Saxne T, van De Loo FA, Heinegard D, van Den Berg WB. IL-1 alpha beta blockade prevents cartilage and bone destruction in murine type II collagen-induced arthritis, whereas TNF-alpha blockade only ameliorates joint inflammation. J Immunol. 1999; 163:5049–5055. [PubMed: 10528210]
36. Braun T, Zwerina J. Positive regulators of osteoclastogenesis and bone resorption in rheumatoid arthritis. Arthritis Res Ther. 2011; 13:235. [PubMed: 21861862]
37. Lam J, Takeshita S, Barker JE, Kanagawa O, Ross FP, Teitelbaum SL. TNF-alpha induces osteoclastogenesis by direct stimulation of macrophages exposed to permissive levels of RANK ligand. J Clin Invest. 2000; 106:1481–1488. [PubMed: 11120755]

38. Kotake S, Sato K, Kim KJ, et al. Interleukin-6 and soluble interleukin-6 receptors in the synovial fluids from rheumatoid arthritis patients are responsible for osteoclast-like cell formation. J Bone Miner Res. 1996; 11:88–95. [PubMed: 8770701]
39. Li J, Sarosi I, Yan XQ, et al. RANK is the intrinsic hematopoietic cell surface receptor that controls osteoclastogenesis and regulation of bone mass and calcium metabolism. Proc Natl Acad Sci U S A. 2000; 97:1566–1571. [PubMed: 10677500]
40. Ling S, Cheng A, Pumpens P, Michalak M, Holoshitz J. Identification of the rheumatoid arthritis shared epitope binding site on calreticulin. PLoS One. 2010; 5:e11703. [PubMed: 20661469]
41. Schett G. Effects of inflammatory and anti-inflammatory cytokines on the bone. Eur J Clin Invest. 2011; 41:1361–1366. [PubMed: 21615394]
42. de Punder YM, van Riel PL. Rheumatoid arthritis: understanding joint damage and physical disability in RA. Nat Rev Rheumatol. 2011; 7:260–261. [PubMed: 21532640]
43. de Almeida DE, Ling S, Holoshitz J. New insights into the functional role of the rheumatoid arthritis shared epitope. FEBS Lett. 2011; 585:3619–3626. [PubMed: 21420962]
44. Holoshitz J, De Almeida DE, Ling S. A role for calreticulin in the pathogenesis of rheumatoid arthritis. Ann N Y Acad Sci. 2010; 1209:91–98. [PubMed: 20958321]
45. Padyukov L, Silva C, Stolt P, Alfredsson L, Klareskog L. A gene-environment interaction between smoking and shared epitope genes in HLA-DR provides a high risk of seropositive rheumatoid arthritis. Arthritis Rheum. 2004; 50:3085–3092. [PubMed: 15476204]
46. Naveh S, Tal-Gan Y, Ling S, Hoffman A, Holoshitz J, Gilon C. Developing potent backbone cyclic peptides bearing the shared epitope sequence as rheumatoid arthritis drug-leads. Bioorg & Medicinal Chem Lett. 2012; 22:493–496.
47. Ollier WE, Harrison B, Symmons D. What is the natural history of rheumatoid arthritis? Best Pract Res Clin Rheumatol. 2001; 15:27–48. [PubMed: 11358413]
48. Korendowych E, Dixey J, Cox B, Jones S, McHugh N. The Influence of the HLA-DRB1 rheumatoid arthritis shared epitope on the clinical characteristics and radiological outcome of psoriatic arthritis. J Rheumatol. 2003; 30:96–101. [PubMed: 12508396]
49. Chan MT, Owen P, Dunphy J, et al. Associations of erosive arthritis with anti-cyclic citrullinated peptide antibodies and MHC Class II alleles in systemic lupus erythematosus. J Rheumatol. 2008; 35:77–83. [PubMed: 18085741]
50. Marotte H, Farge P, Gaudin P, Alexandre C, Mougin B, Miossec P. The association between periodontal disease and joint destruction in rheumatoid arthritis extends the link between the HLA-DR shared epitope and severity of bone destruction. Ann Rheum Dis. 2006; 65:905–909. [PubMed: 16284099]

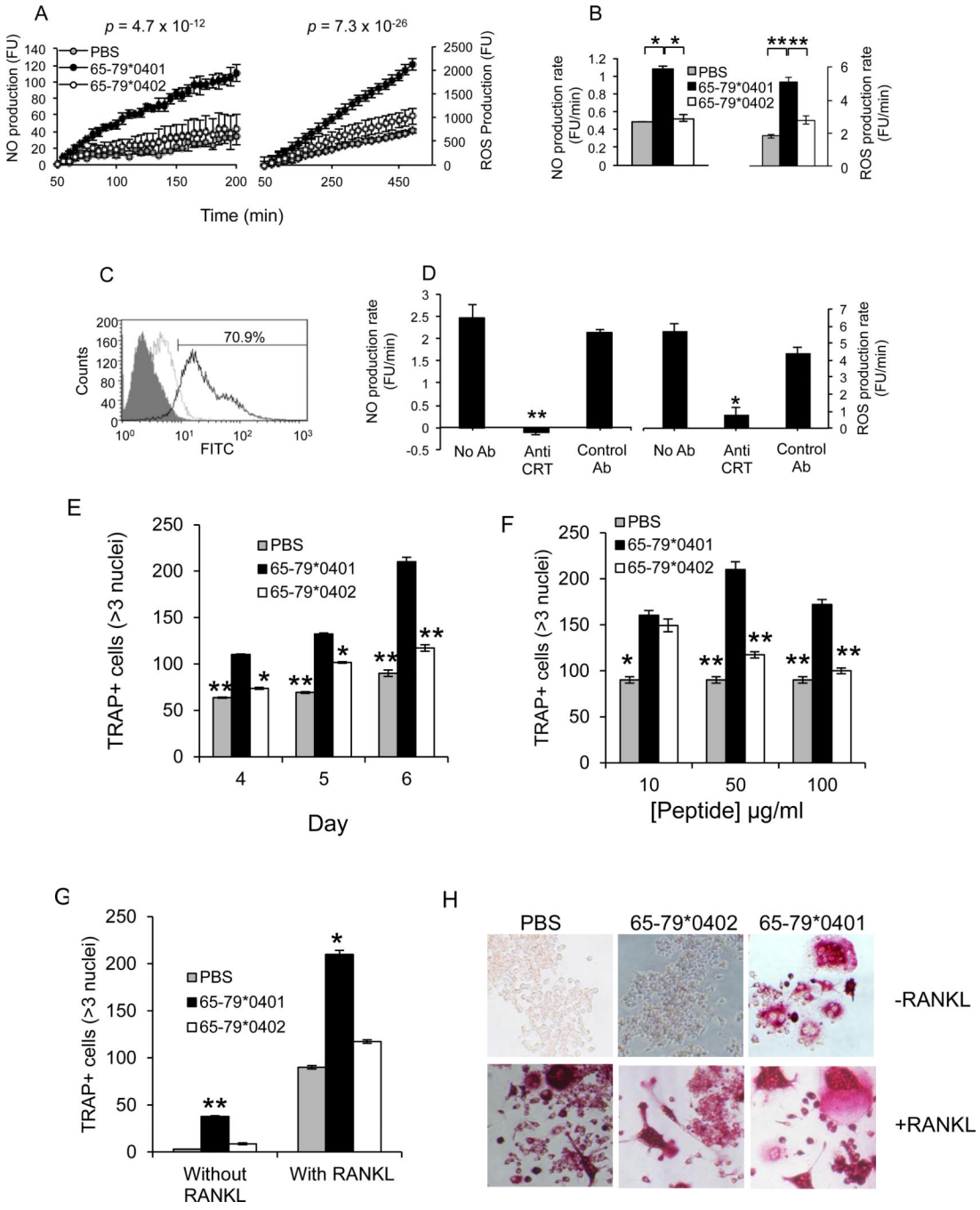

Figure 1. Activation of signaling and OC differentiation by the SE in pre-OCs

(**A**) RAW 264.7 cells (3×10^4 /well) were plated in flat-bottom 96-well plates and treated with or without 50 µg/ml of the SE ligand 65-79*0401, or a SE-negative control peptide 65-79*0402. Data are expressed as the mean ± SEM fluorescence units (FU) in triplicate wells. *P* values were calculated using a paired *t*-test. (**B**) Rates of NO and ROS production (FU/min) in RAW 264.7 cells, cultured as in A. (**C**) Flow cytometric analysis of CRT surface expression in RAW 264.7 cells. Cells were labeled first with either rabbit anti-mouse CRT antibody (solid line), or rabbit anti-mouse control antibody (dashed line), followed by FITC anti-rabbit IgG Ab. The gray-colored histogram represent second-stage antibody only.

(**D**) RAW 264.7 cells were cultured as in A*,* in the presence or absence of rabbit anti-mouse CRT antibodies (1:100), or rabbit anti-mouse, BCL – X s/l (S-18) polyclonal Ig (1:100) as control. NO and ROS production rates were calculated as above. (**E**) RAW 264.7 cells were cultured with M-CSF and RANKL in the presence of 50 μg/ml of the SE ligand 65-79*0401, a SE-negative control peptide 65-79*0402, or PBS for different periods of time. (**F**) RAW 264.7 cells, cultured with M-CSF and RANKL were treated with various concentrations of the SE ligand 65-79*0401, SE-negative control peptide 65-79*0402, or with PBS. (**G** and **H**) RAW 264.7 cells, cultured with M-CSF in the presence or absence of RANKL were treated with the SE ligand, a control peptide, or PBS for 6 days. In all experiments, TRAP-positive multinucleated OCs (>3 nuclei) were counted microscopically. (**H**) Representative microscopic views of the experiment shown in G.

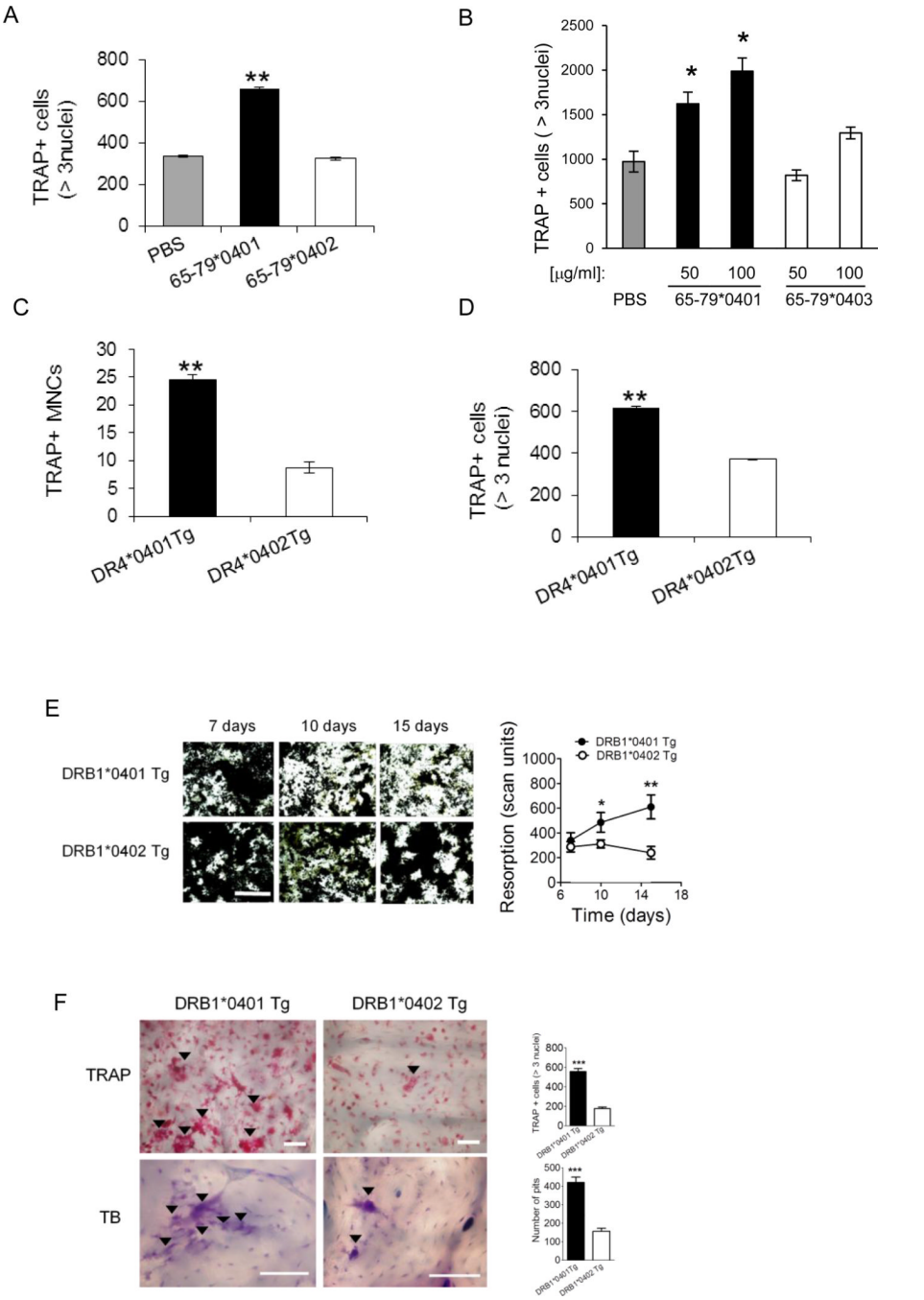

Figure 2. Osteoclastogenic effects of SE in primary cells

(**A**) BMCs harvested from DBA/1 mice were cultured with M-CSF and RANKL in the presence of 50 μg/ml of the SE ligand 65-79*0401, a SE-negative control peptide 65-79*0402, or PBS for 6 days, and TRAP-positive cells counted. (**B**) OCs were differentiated from human PBMCs for 7 days in the presence or absence of the SE ligand 65-79*0401, or a SE-negative control peptide 65-79*0403. (**C**) BMCs from DR4*0401 Tg and DR4*0402 Tg mice in medium without growth factors were allowed to adhere to culture wells overnight and the number of TRAP-positive mononuclear pre-OC cells (MNCs) per well was determined. (**D**) BMCs from DR4*0401 Tg and DR4*0402 Tg mice were cultured

for 6 days OC-differentiating conditions, and TRAP-positive multinucleated cells were counted. (**E**) BMCs from DR4*0401 Tg and DR4*0402 Tg mice were cultured atop bone matrices in OC-differentiating conditions and matrix resorption was quantified at different time points. Black areas represent intact matrix; white areas correspond to matrix resorption. Right hand side shows quantitative data of mean ± SEM of matrix resorption. (**F**) BMCs from DR4*0401 Tg and DR4*0402 Tg mice were cultured atop bone slices in OC-differentiating medium. On day 10, slices were stained for TRAP (upper panel). Arrowheads point at representative OCs. Lower panel shows toluidine blue (TB)-stained bone slices after removal of attached BMCs. Arrowheads point at representative resorption pits. White horizontal bars = 100 μM. Bar graphs in the right hand side represent mean ± SEM events from quintuplicate cultures in each of the two respective panels.

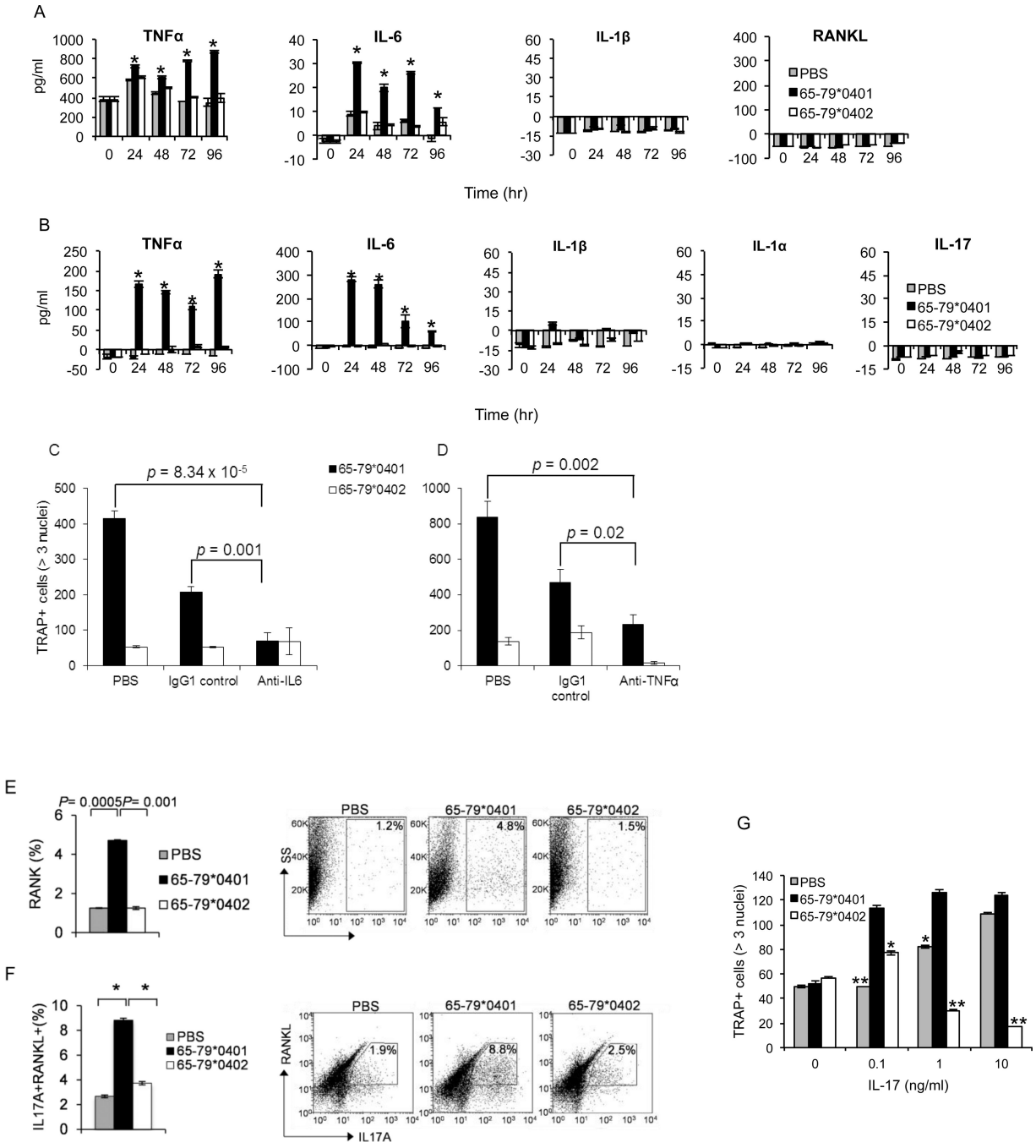

Figure 3. The SE stimulates pro-osteoclastogenic factors

(**A**) RAW 264.7 cells, cultured under OC differentiating conditions as above were treated with 50 μg/ml of the SE ligand 65-79*0401, SE-negative control peptide 65-79*0402, or with PBS. Supernatants were collected at different time points and assayed for cytokines by ELISA. (**B**) BMC from DBA/1 mice, cultured under OC differentiating conditions were treated and cytokines were quantified in the supernatants as in A. (**C** and **D**) BMCs from DBA/1 mice were cultured under OC-differentiation conditions as above in the presence of 50 μg/ml of the SE ligand 65-79*0401, or a SE-negative control peptide 65-79*0402. Rat anti IL-6 (10μg/ml) (C) or anti-TNF-α (5 μg/ml) (D) monoclonal antibodies were added to

respective wells. Rat monoclonal IgG1 was used as a control antibody. After 6 days, cells were stained and OCs were counted. (**E**) RAW 264.7 cells were cultured under OC-differentiating conditions as above in the presence or absence of 50 μg/ml of the SE ligand 65-79*0401, a SE-negative control peptide 65-79*0402, or with PBS. After 6 days, cells were harvested, and RANK surface expression was determined by flow cytometry. (**F**) DBA/1 splenocytes were cultured under Th17-differentiating conditions in the presence or absence of 50 μg/ml of the SE ligand 65-79*0401, a SE-negative control peptide 65-79*0402, or PBS for 5 days. Expression levels of surface RANKL and intracellular IL-17A were determined by flow cytometry. *Left panels*, Bar graphs show the data as percentage (mean ± SEM). *Right panels*, Dot plots of representative experiments. (**G**) BMCs harvested from DBA/1 mice were isolated and cultured for 6 days with M-CSF (10 ng/ml) and a sub-optimal concentration of RANKL (5 ng/ml), in the presence or absence of 50 μg/ml of the SE ligand 65-79*0401, a SE-negative control peptide 65-79*0402, or PBS, in the presence or absence of low concentrations of rmIL-17. TRAP-positive OCs were counted microscopically.

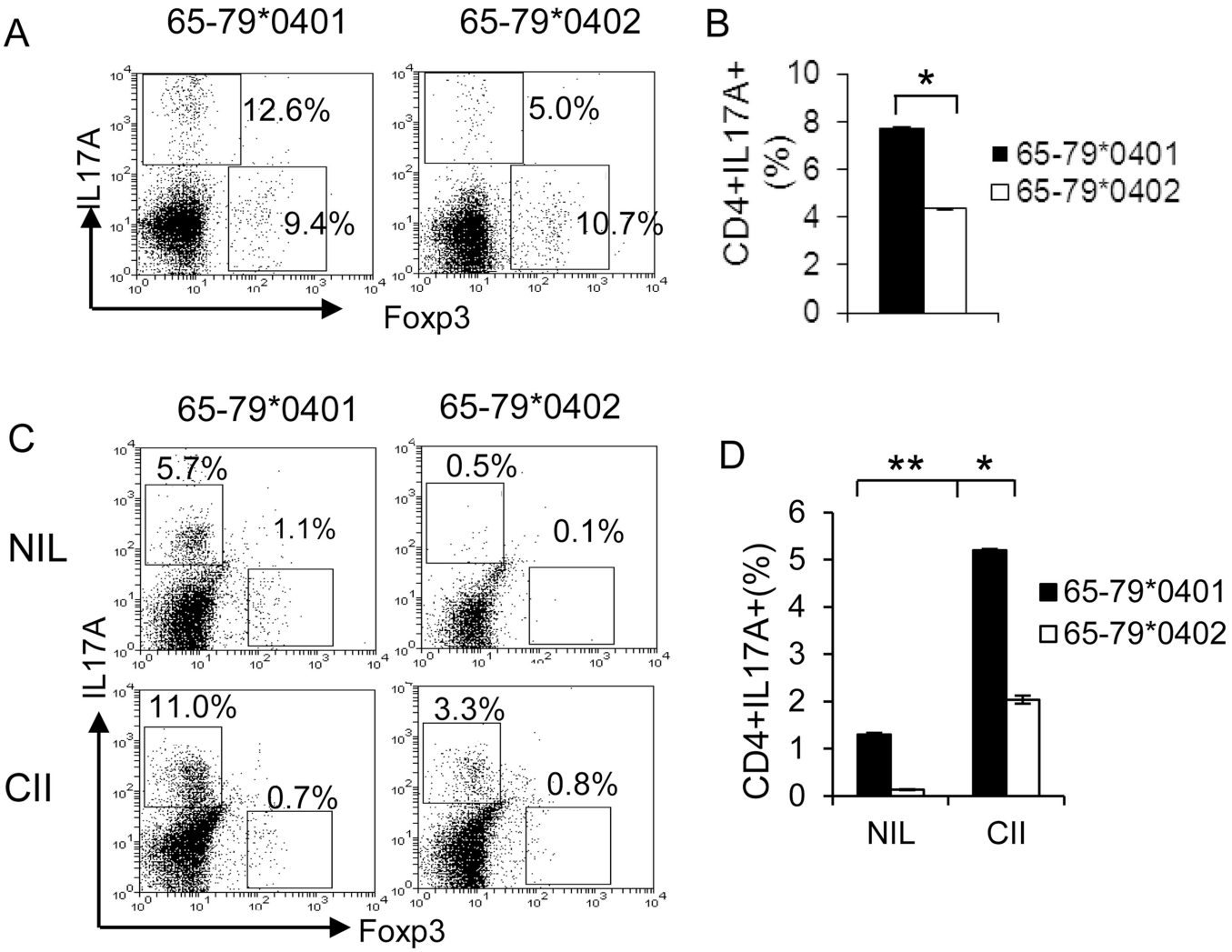

Figure 4. The SE facilitates CII-specific Th17 polarization in CIA mice

Popliteal and inguinal lymph nodes from CIA mice (DBA/1 CII-TCR Tg) treated intraperitoneally with the SE ligand 65-79*0401 or a SE-negative control peptide 65-79*0402. (**A** and **B**) Freshly isolated lymph node cells were cultured for 6 h with PMA, ionomycin and Brefeldin A, and then stained with anti-mouse CD4, IL-17A and Foxp3. (**C** and **D**) Lymph node cells were re-stimulated *ex-vivo* for 5 days with chicken CII (100 μg/ml) or PBS (NIL). *Left panels*, Representative dot plots show percentages of $IL17A^+$ and $Foxp3^+$ cells in gated CD4+ cells. *Right panels*, Bar graphs in B and D show compiled results as mean ± SEM (n = 8).

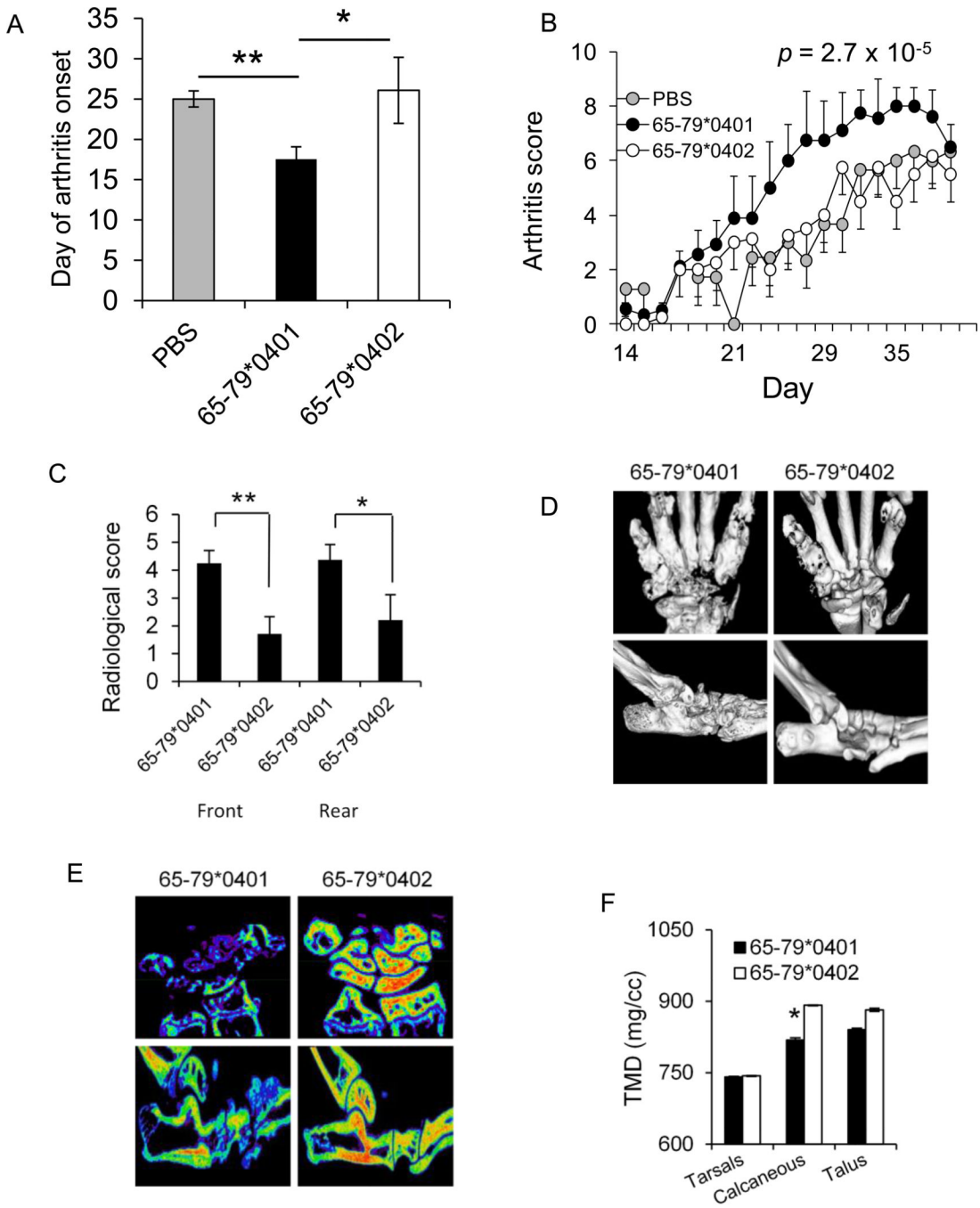

Figure 5. The SE ligand enhances arthritis and bone damage *in vivo*

CIA mice (DBA/1 CII-TCR Tg) were injected intraperitoneally with the SE ligand 65-79*0401, a SE control peptide 65-79*0402 or PBS. Data in A, and B represent compiled results from 2 experiments, n = 28. (**A**) Mean day of arthritis onset. (**B**) Arthritis scores. *P* value represents analysis of 65-79*0401 versus 65-79*0402 in a paired Student *t* test. A comparable level of significance was found in the analysis of 65-79*0401 versus PBS groups. (**C**) Radiological scores of rear and front paws (n = 6) of CIA mice treated with the SE ligand 65-79*0401, or the SE-negative control peptide 65-79*0402. (**D**) Representative ankle and wrist micro-CT images of CIA mice as in C. (**E**) Micro-CT alpha blend images

showing bone mineral content (green = none, blue = lowest, red = highest). (**F**) Quantitative measurement of tissue mineral density (TMD) ± SEM in the two CIA groups (n = 5 per group).

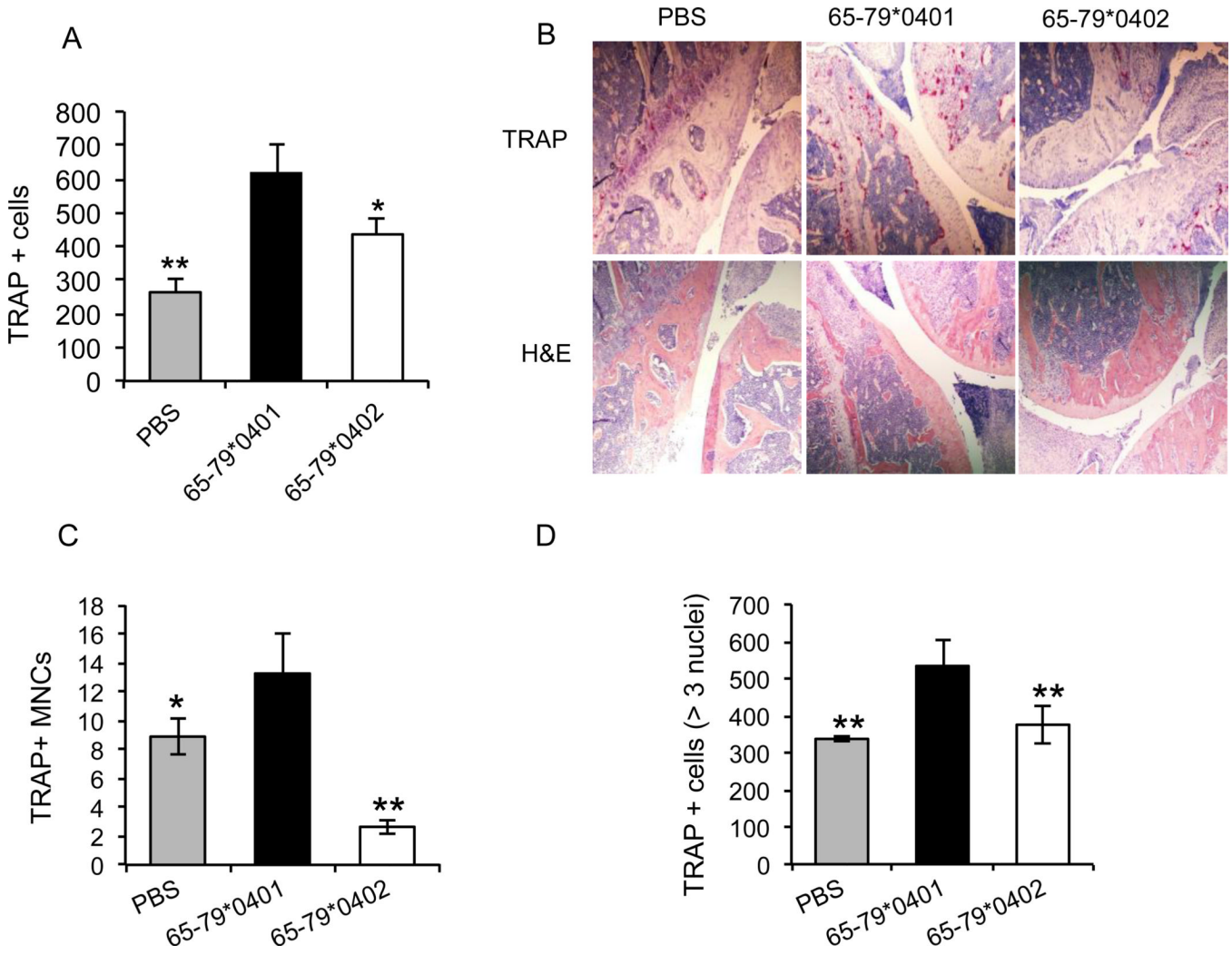

Figure 6. The SE activates osteoclastogenesis *in vivo*

SE ligand 65-79*0401 or control treatments were administered intraperitoneally to CIA mice (DBA/1 CII-TCR Tg). (**A**) Quantification of TRAP-positive cells in CIA joint tissues. (**B**) Representative views of TRAP and H&E-stained knee joint tissue sections of CIA mice. Magnification: × 10. (**C**) Fresh bone marrow cells harvested from CIA mice were analyzed for the abundance of pre-OCs. (**D**) Bone marrow cells harvested from CIA mice were cultured for 6 days under OC-differentiating conditions and OCs were quantified as above.

Table 1

Specificity of SE effect

Peptide (50 μg/ml)	AA Sequence	SE motif	OCs* per well (Mean ± SEM)	*P* value
none	N/A	N/A	444 ± 32	
65-79*0401	KDLLE**QKRAA**VDTYC	+	766 ± 21	**0.001028**
65-79*0402	KDILEDERAAVDTYC	−	395 ± 13	0.131824
65-79*0403	KDLLEQRRAETVDYC	−	407 ± 17	0.191002
65-79*0404	KDLLE**QRRAA**VDTYC	+	661 ± 32	**0.004389**
5-mer peptide #: 1	**RRRAA**	+	725 ± 29	**0.001569**
2	DRRAA	−	385 ± 31	0.13061
3	ERGEP	−	451 ± 22	0.430697
4	**QKRAA**	+	764 ± 28	**0.000922**
5	RTETA	−	391 ± 37	0.169652
6	QRETA	−	417 ± 22	0.262764
7	QARAA	−	455 ± 19	0.397041
8	QKRGR	−	412 ± 44	0.295083
9	RRRAE	−	482 ± 39	0.246378
10	DERAA	−	408 ± 20	0.201715
11	QRRAE	−	496 ± 19	0.124987

*Multinucleated TRAP + cells